

# Progressive Collapse of the World Trade Centre: a Simple Analysis

K. A. Seffen\*

T: +44 1223 764137; F: +44 1223 332662; E: kas14@cam.ac.uk

## Abstract

The collapse behaviour of the World Trade Centre (WTC) towers is considered formally as a propagating instability phenomenon. The application of associated concepts enables the residual capacities of both towers after the onset of collapse to be formally estimated. This information is combined into a simplified variable-mass collapse model of the overall dynamical behaviour. The resulting, non-linear governing equation of motion can be solved in closed form, to yield compact information about the overall collapse conditions.

**Keywords:** progressive failure, residual strength, dynamic analysis

## Introduction

The collapse of the World Trade Centre (WTC) towers on 11 September 2001 was a devastating, catastrophic event. Those factors responsible for the onset of collapse are now well established. Despite localised and substantial horizontal impacts by fuel-laden aircraft, both towers survived until the intense fire compromised the ability of the remaining, in-tact columns close to the aircraft impact zones to sustain the weight of the buildings above them. The subsequent near free-falling of these upper parts over the height of just one storey resulted in dynamical “over-loading” of the relatively undamaged lower columns by a factor of 30 compared to their static load capacity, according to Bažant and Zhou (2002). They argue that the storey immediately below bears the brunt in terms of a localised, plastic

---

\*Lecturer, Structures Group, Department of Engineering, University of Cambridge, Trumpington Street, Cambridge, CB2 1PZ.

buckling of its columns, and they show that the commensurate dissipation cannot arrest the motion of the falling part, leading to a sustained collapse.

This paper examines the collapse sequence by referring the behaviour to concepts familiar in studies on *propagating instabilities*. Such studies usually deal with *progressive collapse* of structures, where damage accrues in a prescribed fashion following an initiation phase. Depending on the local collapse behaviour inveigled by the instability sweeping through the initially undamaged structure, it becomes possible to ascertain the level of loading required to sustain its propagation, or conversely, to quantify the ability of the structure to resist or comply with collapse, thereby defining its “residual capacity”. In the case of the WTC towers, it is clear that the initial loads imposed by both parts falling onto the undamaged buildings beneath were exceptionally high due to the unforeseen preceding events, and that damage was bound to propagate into the floors below: this is the initiation phase. It is also clear that both collapse modes were progressive, as indicated by film footage: there was the sound of each successive impact of floor upon floor and a matching sequence of lateral ejection of debris. Therefore, it is valid to consider the behaviour formally in the proposed terms, and in doing so, the aims of this paper are twofold.

First, this paper aims to show that progressive collapse confers a *substantial* reduction in the performance of the undamaged building compared to its static strength *after* the onset of failure. Other, insightful studies on the WTC towers have estimated this capacity by informal methods, usually by comparing the rate of energy dissipated by the collapsing members to the rates at which the falling parts acquire kinetic energy and lose gravitational potential energy. In terms of progressive behaviour, the attention is confined to the localised collapse of a given storey, which confirms for both WTC towers that there was insufficient residual capacity to arrest this particular type of collapse mode (Bažant and Zhou 2002). However, the link to progressive collapse is improperly asserted by claiming that, because

each storey locally collapses in an unstable manner, successive storeys are bound to fail sequentially (Zhou and Yu 2004). This claim is partially true, but it must also account for the transfer of loading between storeys, which is defined by the final stages of storey collapse. By implementing a simple interpretation here, it becomes rather straightforward to compute the residual capacity of the undamaged building in the proper sense of progressive collapse.

The second aim is to formulate a compact dynamical model of the progressive collapse of the overall building. Even though at any time, the building falls by the columns failing discretely but uniformly within a single storey, a propagating instability viewpoint ensures that the behaviour is independent of the particular snap-shot of current deformation. Accordingly, the assumption of progressive collapse enables a *continuum* viewpoint, which permits a simpler formulation compared to, say, a finite element analysis. Moreover, a closed-form solution becomes available here, which imparts essential transparency to the conditions governing collapse progression: conversely, it is possible to elucidate the conditions required for arresting dynamical collapse, in view of the design and/or retro-fitting (Newland and Cebon 2002) of safer multi-storey buildings.

## Propagating Instabilities

Propagating instabilities feature in structures that are failing progressively. A highly deformed, localised region —the instability— is driven along the structure from the site of first damage, often at a load value below the damaging threshold. They are observed, for example, in the plastic collapse of long pipelines (Kyriakides 1994), where a discrete indentation can spread along the entire length. A frivolous but useful analogue is the inflation of a rubber party balloon: personal experience suggests that a higher lung pressure is required to motivate inflation than that needed to sustain it; and that the latter pressure is approximately constant and steady for a long, uniform balloon, irrespective of the inflated volume

before becoming fully inflated. These two pressures can be identified in Fig. 1 from the typical inflation response for the *overall* balloon. The initial over-pressure is denoted as  $P_{\max}$ , and the steady-state propagation pressure is labelled  $P^*$ .

The peak pressure is identically and more simply calculated from the *uniform* expansion of a cylindrical segment of balloon. The complete response of this segment is also shown in Fig. 1 for a typical non-linear constitutive behaviour belonging to rubber materials. The large changes in geometry also ensure that, beyond the peak value, the overall response is highly non-linear. The precise variation does not matter, but it must exhibit a characteristic *up-down-up* profile, for this enables two areas,  $A_1$  and  $A_2$ , to be respectively enclosed above and below the horizontal line of  $P^*$ , as illustrated. The purpose in doing so, as detailed originally by Chater and Hutchinson (1984), leads to the *Maxwell Construction*, where the exact value of  $P^*$  equates  $A_1$  and  $A_2$ . The underlying hypothesis expresses the equality of two energetic processes: the work done by the pressure in expanding the segment of balloon from a volume  $V_U$  to  $V_D$  (equal to the area under the local pressure curve between the same limits) and the steady-state effort of the propagating front absorbing the same expansion under constant  $P^*$  as the bulge front moves along the balloon.

The Maxwell Construction also applies to other loading cases where the generalised equilibrium response of a small unit of structure exhibits a similar up-down-up feature. If there is plasticity involved, then recovering deformations is not possible: application of the Maxwell Construction is still valid provided the effort, or accumulation of strain energy, is not path-dependent (Chater and Hutchinson 1984) and, crucially, the generic up-down-up character is maintained by the equilibrium path.

Collapse begins when the applied loading surpasses the peak capacity. The location of the initiation site depends on the application of loading, the degree of material uniformity and the boundary conditions: with a balloon, a bulge usually forms at the opposite end, furthest away from the holding

constraints of the inflating device. For both WTC towers, the distributed nature of the aircraft impact sites resulted in a reduced but uneven cross-sectional stiffness over several floors due to differing degrees of missing and deteriorating material. As the most severely affected columns gave way at one level within the impact site, the upper parts fell onto an already weakened cross-section compared to the rest of the building further below. The resulting impingement produced peak forces correctly identified by Bažant and Zhou (2002) to be far in excess of the design capacity of these columns and hence, above the expected value of “ $P_{\max}$ ” (Fig. 1) that could be reasonably carried by them, even if perfect and undamaged. These columns began to deform plastically, thereby seeding failure of this, next part of the structure.

In order to assert the potential for progressive collapse, it is essential to consider the deformation of the next “unit” of structure. This unit is taken to be a single storey whose top and bottom floors laterally restrain the outer columns: compression of the storey follows from the plastic buckling of these columns, as proposed by Bažant and Zhou (2002). All columns are assumed to deform axially and in unison, in a linear one-dimensional way, and the behaviour of a single column is sufficient to characterise the complete response of a storey: the initial softening during buckling of a given column, predicted momentarily via Fig. 2, would suggest a redistribution of load paths into any of the stronger, undeformed columns, which guarantees their buckling and some sense of synchronicity of deformation throughout the storey.

There are three idealised deformation stages for each column shown in Fig. 2: (a) a limited axial shortening; (b) a large-range post-buckling after the formation of discrete plastic hinges; (c) contact, or interference, in which the top and bottom floors coalesce under maximum axial compression. Stages (a) and (b) are replicated from Bažant and Zhou, and their respective performances in terms of a dimensionless compressive force,  $\bar{P}$ , and axial compression,  $\bar{u} = u/l$ , where  $l$  is the storey height, are also

displayed in Fig. 2. Stage (a) is approximately flat as it represents plastic yielding (or elastic buckling) at constant load. Thereafter, rotational hinges of fully plastic moment,  $M_P$ , couple to a significant relative displacement between the floors, to produce a non-linear softening, which is identically expressed by Bažant and Zhou (2002)

$$\bar{P} = \frac{1}{\sqrt{1 - (1 - \bar{u})^2}} \quad (1)$$

where dimensionless  $\bar{P} = Pl/4M_P$ . The final stage, (c), is suggested here, in order to capture the rigid contacting phase when the top and bottom floors come together, and the chosen vertical line neglects any stiffness of the floors in compression. Importantly, stage (c) imparts the rising tail-end to the equilibrium load-path required by the Maxwell Construction, which leads to the existence of “ $P^*$ ”, the equivalent steady-state propagation force outlined in Fig. 1. This force defines the magnitude of the applied loading required to sustain compression of successive storeys; as a corollary, the ability of successive storeys to resist the gravitational and inertia forces imposed upon them by the falling part is governed by the propagation force that they can individually mete.

The calculation of  $P^*$  is found by searching for a horizontal bisecting line in which  $A_1$  equals  $A_2$ . If the contribution from stage (a) is ignored for it persists only up to  $\bar{u} = 3\%$  (Bažant and Zhou 2002), this calculation makes sole use of Eqn 1 more elegantly:

$$\int_0^1 (\bar{P} - \bar{P}^*) d\bar{u} = 0 \quad \Rightarrow \quad \bar{P}^* = \int_0^1 \frac{d\bar{u}}{\sqrt{1 - (1 - \bar{u})^2}} = \frac{\pi}{2} \quad \Rightarrow \quad P^* = \frac{4M_P \bar{P}^*}{l} = \frac{2\pi M_P}{l} \quad (2)$$

By discounting stage (a) and  $P_{\max}$  in this calculation, the true value of  $\bar{P}^*$  is marginally smaller than  $\pi/2$ . Replacing the upper limit of integration by a parameter,  $\xi$ , it is straightforward to show that  $\bar{P}^*$

is modified to

$$\bar{P}^* = \frac{1}{\xi} \left[ \arcsin(\xi - 1) + \frac{\pi}{2} \right] \quad (3)$$

where  $\xi$  can take a value less than unity (but  $\geq 0$ ) to reflect an earlier contact between floors by way, say, of the finite thickness of crushed columns and floors. For example, when  $\xi$  is set to 0.5, *i.e.* 50% compaction,  $\bar{P}^*$  increases by one-third relative to  $\pi/2$ , its value at maximum storey compression. The true value of  $\xi$  is difficult to estimate, but something of the order of 0.8-0.9 becomes acceptable when considering that the columns are hollow sections and the floors are lightweight space-frames, and Fig. 3 indicates a marginal increase in  $\bar{P}^*$  of 5-10% above  $\pi/2$ .

Importantly, the absolute value of  $P^*$  compared to  $P_{\max}$  defines a relative measure of the residual progressive capacity compared to the maximum static strength. A conservative estimate of the latter is the squash load,  $P_Y$ , equal to  $A\sigma_Y$ . Taking the cross-section of column to be a thin-walled box-column (as in the WTC towers) of side-length,  $b$ , and wall thickness,  $t$ , then its area,  $A$ , and plastic section modulus,  $Z_P$ , are approximately  $4bt$  and  $3b^2t/2$ , respectively. It can be verified that

$$\frac{P_Y}{P^*} = \frac{4\Lambda}{3\pi} \quad (4)$$

where  $\Lambda = l/b$  is a slenderness ratio for the column, equal to  $3.68/0.356 \approx 10$ , using WTC column data from Omika et al. (2005). Therefore, the magnitude of the ratio in Eqn 4 is about four, which persists for all columns within a single storey, and the curve in Fig. 2 is simply multiplied by a vertical scaling factor equal to the number of columns distributed within a storey. *Consequently, the residual capacity under progressive collapse is, at best, one-quarter of the peak design force that can be carried quasi-statically by a single storey of columns.* This value does not depend on the Young's modulus,  $E$ , or the

yield stress,  $\sigma_Y$ , of material due to the proposed mode of individual storey collapse, where it is assumed that the material properties retain their design values; if the material strength has been compromised, then the magnitude of softening stage (b) in Fig. 2 is reduced, which lowers  $P^*$ . Alternatively, if the peak capacity depends upon elastic Euler buckling before being followed by the same discrete plastic hinge mechanism, the ratio of peak to propagation forces for the same box column can be calculated as

$$\frac{P_B}{P^*} = \frac{2\pi E}{\Lambda \sigma_Y} \quad (5)$$

where  $P_B$  is four times Euler's value due to the column ends being restrained from rotation by the top and bottom floors. The magnitude of this ratio can be very large, but elastic buckling of the relatively stocky WTC box columns is unlikely. Instead, Bažant and Zhou (2002) suggest that, more realistically, the columns fracture under very little bending immediately beyond the squash load, thereby removing the softening phase altogether in Fig. 2. The Maxwell Construction can still be performed by noting that stage (b) is a vertical step-change from the peak force to zero at the onset of plastic hinge formation, when  $\bar{u} = 3\%$ , resulting in a much lower residual capacity of  $P^* = 0.03P_{\max}$ . This value may be lower still for, consequential to the assumption of column fracture, it is likely that some of the columns do not impinge directly upon undamaged columns below, rather, they pierce the adjacent lightweight space-truss floor, which offers relatively little resistance.

It is clear that the capacity of both buildings, after collapse has begun, is significantly reduced compared to their peak capabilities. In other studies of collapse phenomena, confirmation of this reduction can be ascertained by performing careful experiments in which the instability propagates quasi-statically, without inertial effects, for example by controlling the applied inflation pressure in balloons/pipelines (Kyriakides 1994). In the present case, the unconstrained motion of the falling parts produces time-dependent loading conditions. The ability of the building to resist collapse in an *overall*



sense is inextricably linked to this dynamical performance, whose character, in turn, is concomitant to the magnitude of the propagation force. Thus, confirmation of the calculations of  $P^*$  can be borne out of the properties of dynamical collapse, provided the resulting model is sufficiently robust. In the following section, a simplified but robust model of behaviour is presented. A key feature is that the collapse progression is treated from a continuum viewpoint, where the instability moves continuously down through the structure. The justifiable reasons are twofold: the Maxwell Construction asserts the same  $P^*$  at any point in the deformation of a single storey; each storey is less than 1/100 of the overall building height, the transition region between damaged and undamaged material is very small, and the performance is essentially elemental in nature.

## Dynamical Model of Collapse

The linear, one-dimensional collapse of an homogeneous multi-storey building is shown schematically in Fig. 4. Lateral stability is not considered in view of the near vertical collapse of both WTC towers. Initially, the overall height is  $L$  and the uniform density is  $\rho_0$ . Thereafter, the horizontal level at which the first columns lose strength, due to fire or otherwise, is located at a distance  $\lambda L$  from the top, where  $\lambda < 1$ , see Fig. 4(a). The building everywhere above this floor begins to accelerate downwards as a rigid undamaged body when, at time  $t = 0$ , it impinges on the floor and columns beneath, which are assumed to fail in the manner proposed in the previous section. The instability is formed as a level “crushing front”, its propagation is compatible with the uniform compression of successive storeys, and its precise location lies at a time-varying depth,  $\beta L$ , relative to the initiation floor as shown in Fig. 4(b). Each storey is assumed to compress homogeneously such that the overall “wake” above the crush-front and below the initiation site has a larger, uniform density,  $\rho = r\rho_0$ , compared to the original building, wherein  $r$  is a specified constant greater than unity.

The velocity,  $v$ , of the moving parts is established from the incremental compression displayed in Figs 4(c) and (d). At time  $t$ , an elemental mass of undamaged building (a storey, or part thereof) has a height,  $c\delta\beta L$ , and lies just beneath the crush-front. Over a period,  $\delta t$ , the compressed region extends  $\delta\beta L$  by absorbing the same element, whose height reduces by  $(c - 1)\delta\beta L$  as the crush-front passes through it. The constant compression factor,  $c$ , is greater than unity and approximately equal to  $r$ , although it can be calculated with greater precision: note that  $c$  is exactly equal to  $1/(1 - \xi)$ , where  $\xi$  is presented in the previous section and in Fig. 3. In the same time, the falling parts are displaced by  $(c - 1)\delta\beta L$  downwards, and their velocity is

$$v = (c - 1)\dot{\beta}L \quad (6)$$

where an over-dot denotes differentiation with respect to time. If the falling parts have mass,  $m_\lambda$  and  $m_\beta$ , where the subscript refers to the appropriate body by way of its height, then the incremental change in gravitational potential energy,  $V$ , can be simply written as

$$\delta V = -(m_\lambda + m_\beta)g(c - 1)\delta\beta L \quad (7)$$

The minus sign accounts for a release of energy, and  $g$  is the acceleration due to gravity. The Maxwell Construction in the previous section endows the building with a fixed residual capacity under column plasticity effects via  $P^*$ . The resulting, dissipated energy is denoted as  $W$ , where the elemental change,  $\delta W$ , is straightforwardly calculated from the work done over the same increment of displacement

$$\delta W = -P^*(c - 1)\delta\beta L \quad (8)$$

It is tacitly assumed that  $P^*$  is distributed over the entire cross-section at a given height, as shown in

Fig. 4. Finally, the moving parts have the same velocity,  $v$ , and their kinetic energy,  $T$ , can be simply written

$$T = \frac{1}{2}(m_\lambda + m_\beta)v^2 \quad (9)$$

As the crush-front impresses upon undamaged material, mass initially at rest is enveloped by the falling part over a very short distance but in a continuous fashion. Accordingly, there is a narrow transition zone associated with the instability, but its kinetic energy is sufficiently negligible compared to the size of  $T$ . Other sources of strain energy, *e.g.* elastic, are assumed to be negligible or invariant during collapse.

The governing equation of motion is found by application of Lagrange's equation (Greenwood 1997), which can be stated in the following pertinent form for systems of constant mass

$$\frac{d}{dt} \left( \frac{\partial T}{\partial \dot{\beta}} \right) - \frac{\partial T}{\partial \beta} + \frac{\partial V}{\partial \beta} = Q_\beta \quad (10)$$

The generalised coordinate is  $\beta$ , and  $T$  and  $V$  follow straightforwardly after defining  $m_\lambda = \rho_0 \lambda L g$  and  $m_\beta = \rho \beta L g$ , where the “1” deals with unity cross-sectional area for simplicity — the general outcome is not affected. Note that  $m_\beta$  is a function of time due its dependence on  $\beta$ , and hence, there are similarities here to problems involving *variable mass*, for the kinetic- and potential energy expressions strictly apply to the mass of the falling portion alone, which increases over time. Application of Eqn 10 remains valid provided the mass is an explicit function of time whose variation stems from entrainment, or expulsion, of mass at a relative velocity of zero. Although the crush-front absorbs stationary mass,  $m_\beta$  is an explicit function of the spatial coordinate,  $\beta$ , rather than of time, and Pesce (2003) advocates an augmented form of Eqn 10 to reveal the correct governing equation of motion. However, there is

a subtle point to make, for Pesce's modification essentially reconciles the energetic formulation to a Newtonian approach, which equates momentum changes to external impulses, *and* to the underlying assumptions imbued in this approach. Ordinarily, this makes no difference, but it does so in the present case for the crush-front has negligible height: an element of mass is picked up from rest instantaneously as the front moves through it, resulting in a *discontinuous* velocity profile during entrainment. This motion is automatically impulsive, which contravenes any conservative assumption that can be applied to the entrainment conditions; indeed, it predicates *artificial* dissipation by naturally leaking kinetic energy. Dynamics text-books, either purposefully or incidentally, address this point in simpler variable-mass problems by associating this dissipation to physical behaviour. For example, when one end of a linked chain is pulled from without a pile, the links are assumed to acquire velocity through successive and dissipative impacts between stationary and moving links over a very short transition zone. In cases where the physical motion is conservative, *e.g.* where a flexible rope is uncoiled similarly to the linked chain, and the size of any transition zone remains negligible, then a Newtonian approach is not appropriate nor accurate, and a non-dissipative formulation is essential.

Typically, there are two remedies, either: the transition region is specified with a finite height by an extra coordinate, enabling a formulation in which there is a continuous acceleration of entrained/expelled mass; or, application of the original Lagrange's equation is simply upheld without changing the size of the transition zone, in order to pander to the need for conservatism whilst retaining simplicity. If Pesce's modification to Eqn 10 is imported here, there will be an extra term in the governing equation of motion over and above the fundamental form but only because the crush-front has zero height, where the extra term identically equates to artificial dynamical dissipation in the crush-front. Of course, it can be argued that such dissipation introduces a means for capturing dynamical effects arising from, say, column-upon-column impacts, but it is prescriptive rather than attentive in terms of correct amount, which would be

very difficult to estimate. Thus, it is entirely appropriate to move the study forward within the spirit of using Eqn 10 directly, for it is assumed primarily that dissipation is confined to quasi-static deformation in the columns and that the progressive nature of collapse demands a continuous mass entrainment. Beneficially, the resulting equation of motion can be solved in *closed form*, thereby quantifying the generic performance and imparting essential transparency. For completeness, the Newtonian-based equation of motion is presented later and solved numerically, to provide a complementary bound on performance compared to Lagrange: and, as it turns out, the discrepancy between results from both methods is not significant. The reader is directed towards an earlier study by the author (Seffen and Pellegrino 1999) for a wider discussion on this subtle but important issue.

Substituting for each of the mass terms,  $m_\lambda$  and  $m_\beta$ , into Eqn 9, and performing the required differentiation, it can be verified that

$$\frac{d}{dt} \left( \frac{\partial T}{\partial \dot{\beta}} \right) - \frac{\partial T}{\partial \beta} = \rho_0 L^3 (c-1)^2 \left[ (\lambda + r\beta)\ddot{\beta} + \frac{1}{2}r\dot{\beta}^2 \right] \quad (11)$$

The  $\partial V/\partial \beta$  term in Eqn 10 is obtained by dividing Eqn 7 by  $\delta\beta$ , and observing its limit. The generalised dissipative force,  $Q_\beta$ , is calculated from the rate of energy dissipation with respect to the generalised coordinate, *i.e.*  $\partial W/\partial \beta$ , which is found after dividing Eqn 8 by  $\delta\beta$  and also observing its limit. Substituting these terms into Eqn 10 along with Eqn 11, re-arranging and then normalising by dividing by  $m_\lambda g$ , eventually produces

$$\left( \frac{\lambda}{r} + \beta \right) \ddot{\beta} + \frac{1}{2}\dot{\beta}^2 = \frac{\alpha \lambda}{2r} \left( 1 + \frac{r}{\lambda}\beta - p^* \right) \quad \text{with } \alpha = \frac{2g}{(c-1)L}, \quad p^* = \frac{P^*}{m_\lambda g} \quad (12)$$

The above is the non-linear, second-order equation governing the development of the compressed wake and its dynamical motion in concert with the falling upper part during collapse; it is valid until  $\beta$

extends to the bottom of the building, when  $\beta = (1 - \lambda)/c$ . Thereafter, a different formulation is required, which is beyond the scope of this study.

A solution for  $\dot{\beta}$  can be obtained in closed form by re-casting the left-hand side as a first-order, ordinary differential equation by using the relationship

$$\left(\frac{\lambda}{r} + \beta\right) \ddot{\beta} + \frac{1}{2} \dot{\beta}^2 = \frac{1}{2} \frac{d}{d\beta} \left[ \left(\frac{\lambda}{r} + \beta\right) \dot{\beta}^2 \right] \quad (13)$$

Initially,  $\dot{\beta}(0)$  is not zero, for it is determined by the initial impingement conditions of the  $m_\lambda$  portion on the lower part of the building. As argued in Bažant and Zhou (2002), it is likely that the uppermost parts of the WTC towers were falling freely due to an absence of column resistance in the first weakest storey, and that the speeds of impingement were not reduced due to the gross amplification of localised impact forces. Defining the height of a single storey to be  $\gamma L$ , where  $\gamma \ll 1$ , conservative motion of the  $m_\lambda$  block just before  $t = 0$  results in its velocity at the point of impingement, when  $t = 0$ , equal to

$$v(0) = \sqrt{2g\gamma L(c - 1)/c} \quad (14)$$

The crush-front adopts this speed completely and Eqn 6 applies, to reveal

$$v(0)^2 = (c - 1)^2 \dot{\beta}(0)^2 L^2 \quad \Rightarrow \quad \dot{\beta}(0)^2 = \frac{\alpha\gamma}{c} \quad (15)$$

Substituting Eqn 13 into Eqn 12, integrating with respect to  $\beta$  for the above initial conditions, and tidying up, produces

$$\dot{\beta} = \left[ \frac{\alpha}{1 + (r/\lambda)\beta} \cdot \left[ \beta(1 - p^*) + \frac{r}{2\lambda}\beta^2 + \frac{\gamma}{c} \right] \right]^{0.5} \quad (16)$$

For a given value of  $\beta$  in the range 0 to  $(1-\lambda)/c$ , the speed of the crush-front becomes directly available from the above expression, which can be substituted back into Eqn 12 to solve for its acceleration; correspondingly, the velocity and acceleration of the falling parts above, respectively Eqn 6 and its time derivative, can be computed. Another important parameter is the time taken by the crush-front to reach the bottom of the building, for it defines the collapse period,  $\tau$ . This quantity can be found by numerically integrating the following expression, after separating the variables in Eqn 16

$$\tau = \int_{\beta=0}^{\beta=(1-\lambda)/c} \left[ \frac{1}{\alpha} \cdot \frac{1 + (r/\lambda)\beta}{\beta(1-p^*) + (r/2\lambda)\beta^2 + \gamma/c} \right]^{0.5} d\beta \quad (17)$$

In order to predict behaviour, the values of parameters are now cast. The relative height of a single storey is  $\gamma = 1/110$ , and the compression factor,  $c (= r)$ , is taken to be five although there is little variation in the dynamical results provided  $c$  is larger than two.  $L$  is set to be 416 m, the average height of both WTC towers,  $g = 9.81 \text{ m/s}^2$ , and the value of  $\alpha$ , equal to  $2g/(c-1)L$ , follows. In the previous section, the value of  $P^*$  ( $= p^*m_\lambda$ ) was shown to be, at best, not more than one-quarter of the peak design capacity of each storey, although it could be as much as ten times less. Optimistically, setting  $P^*$  equal to the weight of the entire building, then

$$p^* \approx \frac{\rho_0 L g}{R} \cdot \frac{1}{\rho_0 \lambda L g} = \frac{1}{R \lambda} \quad (18)$$

where  $R$  formally denotes the factor by which the peak capacity is reduced, not being smaller than four. The relative heights of the initial falling blocks,  $\lambda$ , are 15/110 for WTC tower 1 (WTC1) and 28/110 for WTC tower 2 (WTC2), which are based crudely on the floor locations of central aircraft impacts, 95 (WTC1) and 82 (WTC2). The respective upper bounds on  $p^*$  are therefore 1.75 and unity, but realistic values are likely to be smaller, and results are presented correspondingly for a range of  $p^*$ .

## Dynamical Predictions

At the start of collapse, the accelerations of the crush-front,  $\ddot{\beta}(0)$ , and the uppermost falling block,  $a(0)$ , are found to be

$$\ddot{\beta}(0) = \frac{g}{(c-1)L} \left(1 - \frac{\gamma r}{\lambda c} - p^*\right), \quad a(0) = \frac{dv(0)}{dt} = (c-1)\ddot{\beta}(0)L = g \left(1 - \frac{\gamma r}{\lambda c} - p^*\right) \quad (19)$$

Given that  $r \approx c$  and  $\lambda/\gamma \gg 1$ , the initial acceleration of the falling part just after it impinges onto the undamaged building is approximately  $g(1 - p^*)$ . This result can be confirmed in Fig. 5, which displays the full range of acceleration, normalised by dividing by  $g$ , for  $0 \leq \beta \leq (1 - \lambda)/c$  using the properties of WTC1. The applicable range of  $p^*$  extends from zero up to a maximum value, at which the velocity of the crush-front becomes zero within the allowable range of  $\beta$ , indicating that collapse has been arrested. If  $p^*$  is set equal to  $1 + \epsilon$  for convenience, the conditions for  $\dot{\beta}$  becoming zero in Eqn 16 are satisfied by the right-hand side being equal to zero, specifically

$$\frac{r}{2\lambda}\beta^2 - \epsilon\beta + \frac{\gamma}{c} = 0 \quad \Rightarrow \quad \beta = \frac{\epsilon\lambda}{r} \left[1 \pm \left(1 - \frac{2\gamma r}{\lambda c \epsilon^2}\right)^{0.5}\right] \quad (20)$$

Real values of  $\beta$  are asserted only when  $\epsilon \geq \sqrt{2\gamma r/\lambda c}$  and thus, the minimum amount of residual capacity required to arrest collapse is

$$p_{\text{arrest}}^* = 1 + \sqrt{\frac{2\gamma r}{\lambda c}} \quad (\text{equal to } 1.37 \text{ for WTC1 and } 1.27 \text{ for WTC2}) \quad (21)$$

If  $p^*$  is smaller than  $p_{\text{arrest}}^*$ , propagation of the instability and collapse are assured. For a value just less  $p_{\text{arrest}}^*$ , the initial acceleration of the falling parts is negative; but, as Fig. 5 attests, a steady-state value emerges irrespective of the value of  $p^*$ , being equal to  $g/2$ . This exact value can be ascertained



by noting that the rate of change of acceleration of the crush-front with its progression is zero, *i.e.*

$d\ddot{\beta}/d\beta = 0$ , which is also satisfied by  $d^2(\dot{\beta}^2)/d\beta^2 = 0$ . Implicit differentiation of Eqn 16 reveals

$$\frac{r}{\lambda} \left[ \dot{\beta}^2 + \beta \frac{d(\dot{\beta}^2)}{d\beta} \right] = \alpha \left( 1 - p^* + \frac{r}{\lambda} \beta \right) \quad (22)$$

and further differentiating once more, results in the solution

$$\ddot{\beta}_{\text{steady}} = \frac{\alpha}{4} \quad \Rightarrow \quad a_{\text{steady}} = \ddot{\beta}_{\text{steady}}(c - 1)L = \frac{g}{2} \quad (23)$$

The reason for the development of a steady-state value is intimately connected to  $p^*$ , even if its value does not affect the general outcome for the range of  $p^*$  considered. If the residual capacity is small and close to zero, then the ability of the falling part to acquire additional mass and kinetic energy is relatively uninhibited. Under conservative conditions, which neglect  $p^*$ , the release of potential energy ensures an uptake of kinetic energy of the falling part but also for the entrained mass, which must be accelerated from zero: the variable-mass nature predicates a decreasing acceleration rate compared to the initial free-fall conditions. This rate, as well as the initial acceleration, are diminished by a non-zero  $p^*$ , but when  $p^* = (1 - \gamma r/\lambda c)/2$  ( $\approx 0.46$  for WTC1), it is readily verified using Eqn 12 that the initial acceleration of the crush-front is immediately equal to  $\ddot{\beta}_{\text{steady}}$  when  $\beta = 0$ , giving way to a constant acceleration throughout. When the residual capacity is larger than  $(1 - \gamma r/\lambda c)/2$ , the rate of acceleration increases from a nominal value below  $g/2$ . Even though the resistance to collapse has increased in an overall sense, locally, there is a comparatively larger force serving to compress each storey, which actively enhances the collapse conditions and the entrainment of mass by the crush-front; but as the mass of the falling part increases, the acceleration rate declines as the relative increase of mass of the falling part attenuates. The particular steady value of  $g/2$  is a consistent property of any

variable-mass system where the mass, initially at rest, is entrained by a non-impulsive action. An exposition of these general cases can be found in any comprehensive dynamics textbook, *e.g.* Meriam and Kraige (2003).

For completeness, Fig. 6 indicates the velocity,  $v$ , of the falling part for the same values of  $p^*$ , relative to the equivalent free-falling velocity,  $v_g$ , equal to  $\sqrt{2g(c-1)L(\beta + [\gamma/c])}$ , for conservative motion over the same vertical displacement  $(c-1)\beta L$ . The actual velocity is Eqn 6, whence

$$\frac{v}{v_g} = \sqrt{\frac{(c-1)L\dot{\beta}^2}{2g(\beta + \gamma/c)}} \quad (24)$$

There are two features to note from Fig. 6. First, the motion exhibits a similar asymptotic behaviour compared to Fig. 5, where  $v/v_g$  tends towards  $1/\sqrt{2}$  commensurate with the steady state acceleration of  $g/2$ , but only when  $p^*$  is small. Second, as the residual capacity increases, the velocity near the start of collapse dips towards zero before rising again. If  $p^*$  is set equal to  $p_{\text{arrest}}^*$ , then zero velocity and collapse arrest occurs at  $\beta$  equal to  $\lambda\sqrt{8\gamma/rc}$  via Eqn 20, equal to 0.012 for WTC1, for  $c = 5$  in this simulation. In other words, the compressed wake is of original height  $5 \times 0.012L$ , which equates to 6-7 storeys.

When collapse is total, Fig. 7 records the time period,  $\tau$ , obtained from Eqn 17, for a continuous variation in  $p^*$  up to  $p_{\text{arrest}}^*$ . Two curves are furnished for each of the WTC towers. The variations rise sharply in both for  $p^*$  approaching  $p_{\text{arrest}}^*$ , as might be expected. However, in the range between zero and unity, the proportional increase is approximately one-half, which can be divined from recalling that the relative acceleration is approximately  $1 - p^*$ , and the corresponding time of motion is proportional to  $1/\sqrt{1-p^*} \approx 1 + p^*/2$ . The actual time for collapse of WTC1 ranges from 8.3 s ( $p^* = 0$ ) to 12.0 s ( $p^* = 1$ ), and for WTC2, from 7.3 s to 12.1 s, for the same range of  $p^*$ . Reassuringly, these limits embrace the observed period for both towers, approximately equal to 11 s, and the residual capacity of

both buildings was indeed limited compared to their best values.

Finally, a second set of curves is also shown in Fig. 7, which stem from a Newtonian-based governing equation of motion. Newton's second law can be applied to the variable-mass sub-system in Figs 4(c) and (d), for the contained mass is constant with respect to the separating but infinitesimal time period,  $\delta t$ . The change in linear momentum can be written as

$$\rho_0 \lambda L \delta v + \rho \beta L \delta v + \rho \delta \beta L v \quad (25)$$

and the corresponding impulse in the same direction is found to be

$$[\rho_0 \lambda L g + \rho \beta L g - P^*] \delta t \quad (26)$$

Equating both expressions, dividing by  $\delta t$  and observing the limit, and re-arranging, leads to the form

$$\left(\frac{\lambda}{r} + \beta\right) \ddot{\beta} + \dot{\beta}^2 = \frac{\alpha \lambda}{2 r} \left(1 + \frac{r}{\lambda} \beta - p^*\right) \quad (27)$$

which differs from Eqn 12 by the term,  $\dot{\beta}^2$ , being pre-multiplied by unity here rather than by one-half, which is equivalent to introducing an extra term,  $\dot{\beta}^2/2$  into the left-hand side of the final Lagrange-based equation. As noted in the previous section, this difference can be traced back to the differences in mass entrainment through a crush-front of negligible height: Lagrange's equation assumes a smooth performance whereas the Newtonian method is impulsive and non-conservative; and Pesce's (Pesce 2003) modified approach to Lagrange would introduce this extra term precisely.

Numerical integration of Eqn 27 is straightforward wherein  $(\beta, t)$  are extracted for the same boundary conditions for both buildings as before. As can be seen in Fig. 7, the period for collapse increases in general by around 10% for all values of  $p^*$ . Hence, the general rapidity of collapse remains unchanged.

## Concluding Remarks

The collapse behaviour of the WTC towers has been compared to the rapid propagation of an instability downwards through both structures. The instability is formed by the dynamical overloading of the storey immediately below the weakened columns surrounding the aircraft impact sites. As this storey locally collapses, the instability moves ahead and below as a level crushing front, leaving behind a compressed wake. The force required to sustain propagation of the instability is obtained from the so-called Maxwell Construction, which has been applied to the large-displacement behaviour of a single storey. It has been shown that this force is much lower than the peak capacity of the undamaged columns within each storey, and that the instability progresses if the forces applied to a given storey exceed the Maxwell value. The corresponding dynamical behaviour of the overall building has been captured by an idealised variable-mass model derived using Lagrange's equation, and its closed-form predictions, which are listed as follows, are simplified by defining a constant,  $\epsilon = \sqrt{2\gamma r/\lambda c}$ . [Recall  $\gamma$  and  $\lambda$  are the relative heights of a single storey and initial falling part;  $c$  and  $r$  are specified compression factors in which  $c \approx r$  and provided  $c \gg 2$ , the results are independent of  $c$ .]

- The initial acceleration of falling parts is equal to  $g(1 - p^* - \epsilon/\sqrt{2})$ , where  $p^*$  is the residual capacity normalised by dividing by the weight of the initial falling part. The local collapse mode, which defines  $p^*$ , follows that from Bažant and Zhou (2002).
- The crush-front will stop moving if  $p^*$  is greater than  $p_{\text{arrest}}^* = 1 + \epsilon$ , with a maximum displacement of  $2\epsilon\lambda/r$ .
- If there is insufficient  $p^*$ , the acceleration of the falling part tends towards a constant value of  $g/2$ , irrespective of  $p^*$ , whilst entraining mass from the undamaged building below. In the early stages, the acceleration rate decreases if  $p^* < (1 - \epsilon^2)/2$ , and *vice versa*: when  $p^* = (1 - \epsilon^2)/2$ ,

the acceleration is constant throughout collapse and equal to  $g/2$ .

- For  $p^*$  smaller than unity, the time taken by the crush-front to reach the base of the building is approximately  $1 + p^*/2$  compared to its free-fall period.
- For the WTC towers, upper estimations of  $p^*$  are 1.75 (WTC1) and unity (WTC2), which presumes that the deforming columns develop fully plastic and ductile rotational hinges. More realistically, if there is column fracture,  $p^*$  is much less than unity. The residual capacities required to arrest collapse are estimated to be 1.37 (WTC1) and 1.27 (WTC2) for the simplified dynamical account here.

Many simplifications have been made in this analysis for the sake of transparency. For example, the constructional properties of original WTC towers are not homogenous over the entire height, but only over discrete portions and differently so. The collapse mode is highly idealised: none of the falling mass moves laterally; any impulsive action between successive floor impacts is neglected; and the final stage of collapse after the crush-front reaches the base is discounted. However, the incorporation of these features into a subsequent model would rely on estimations apportioning their relative contributions, which are not straightforward. Such refinements may negate the ability to obtain closed-form solutions, which are essential in ascribing the generic character of behaviour and for distilling key formulae, especially in view of designing buildings to withstand progressive collapse. Importantly, this study has shown that progressive collapse and its features are concomitant to the full, up-down-up deformation response of the structural unit, and that its properties are finely balanced — that collapse can be total or not at all, and that, in the former case, the rate of collapse tends to a uniform acceleration not dependent on the residual capacity of the building. These comments attest to the similarities between the collapse sequences of both WTC towers despite their quite different initial conditions. And it is noted that progressive collapse, when wrought, is quite ordinary and regular and not due to extraordinary,

possibly conspiratorial, influences.

## **Acknowledgements**

The author is extremely grateful to two anonymous referees for insightful and supporting comments.

## References

- Bažant, Z.P. and Zhou, Y. Why did the World Trade Center collapse? - a simple analysis. *Journal of Engineering Mechanics - ASCE*, 128(1):2–6, 2002.
- Chater, E. and Hutchinson, J.W. On the propagation of bulges and buckles. *Journal of Applied Mechanics*, 51:269–277, 1984.
- Greenwood, D.T. *Classical Dynamics*. Dover, 1997.
- Kyriakides, S. Propagating instabilities in structures. In Hutchinson, J W and Wu, T Y, editor, *Advances in Applied Mechanics*, pages 67–189. Academic Press, 1994.
- Meriam, J.L. and Kraige, L.G. *Engineering Mechanics Volume 2: Dynamics*. Wiley, fifth edition, 2003.
- Newland, D.E. and Cebon, D. Could the World Trade Center have been modified to prevent its collapse? *Journal of Engineering Mechanics - ASCE*, 128(7):795–800, 2002.
- Omika, Y., Fukuzawa, E., Koshika, N., Morikawa, H., and Fukuda, R. Structural responses of the World Trade Center under aircraft attacks. *Journal of Structural Engineering - ASCE*, 131(1):6–15, 2005.
- Pesce, C.P. The application of Lagrange equations to mechanical systems with mass explicitly dependent on position. *ASME Journal of Applied Mechanics*, 70:751–756, 2003.
- Seffen, K.A. and Pellegrino, S. Deployment dynamics of tape springs. *Proceedings of the Royal Society, London, Series A*, 455:1003–1048, 1999.
- Zhou, Q. and Yu, T.X. Use of high-efficiency energy absorbing device to arrest progressive collapse of a tall building. *Journal of Engineering Mechanics*, 130(10):1177–1187, 2004.

## List of Figures

- 1 Pressure-volume response of a long, uniform party balloon. Left: the overall equilibrium path where  $V$  refers to the inflated volume. The volumes,  $V_U$  and  $V_D$ , refer to the volumes of a “unit” length of material in the undeformed region, ahead of the instability (the bulge front), and behind, after gross deformation. Right: the equilibrium response for the uniform, cylindrical inflation of the same unit length of material. The same peak pressure  $P_{\max}$  is manifest, and  $P^*$  is the steady-state force which assures propagation of the bulge, found by setting the enclosed areas,  $A_1$  and  $A_2$ , equal to each other. This procedure is known as the Maxwell Construction. . . . . 26
  
- 2 Large-displacement compression of a column built-in at both ends: (a) axial compression, which can be elastic buckling or plastic squashing, both at constant load; (b) a plastic hinge mechanism, which leads to Eqn 1; (c) a rigid contact between the ends. These stages are summarised schematically on the right in terms of a dimensionless compressive force,  $\bar{P}$ , and axial displacement,  $\bar{u}$ . The Maxwell Construction described in Fig. 1 indicates the dimensionless propagation force,  $\bar{P}^*$ , when  $A_1 = A_2$ . . . . . 27
  
- 3 Variation of propagation force with compaction. The dimensionless force,  $\bar{P}_\xi^*$ , is the force,  $\bar{P}^*$ , from Eqn 3 divided by its value when there is full compaction, *i.e.* when  $\bar{P}^* = \pi/2$ . The dimensionless compaction ratio is  $\xi$ , which describes the relative compression of a single storey, where a value of unity is maximal:  $\xi = 0.5$  implies that the storey is compressed by 50%. . . . . 28



4	<p>Dynamical model of progressive collapse of the overall building. (a) The initial configuration at time <math>t = 0</math>, where the initiation floor corresponds to the level of first damage and hence, the crush-front, located <math>\lambda L</math> beneath the top of the building. (b) The crush-front has propagated <math>\beta L</math> over time <math>t</math>, resulting in motion of the parts above. (c) and (d) offer incremental views of the entrainment and compression of a small element of mass over time <math>\delta t</math>, which acquires the velocity, <math>v</math>, of the falling parts. The resistance to motion is met by the propagation force, <math>P^*</math>, from Fig. 2, and <math>c</math> is a geometrical compression factor.</p>	29
5	<p>Predictions of acceleration, <math>a</math>, of the collapsing building above the crush-front from Fig. 4 for the indicated range of <math>p^* = P^*/m_\lambda g</math>, the ratio of propagation force to the weight of the initial falling part (of relative height <math>\lambda = 15/110</math>, as in WTC1). The final value of <math>p^* = 1 + 3\epsilon/4</math>, where <math>\epsilon = \sqrt{2\gamma r/\lambda c}</math>, is just smaller than the value to cause arrest (<math>p^* = 1 + \epsilon</math>). The maximum value of <math>\beta</math> is <math>(1 - \lambda)/c</math> with <math>c</math> set to five.</p>	30
6	<p>Predictions of velocity of the collapsing building above the crush-front from Fig. 4, for the same initial conditions in Fig. 5.</p>	31
7	<p>Comparison of the time period for collapse, <math>\tau</math>, for both WTC towers (solid, WTC1; dashed, WTC2). The thicker lines refer to solutions derived from Lagrange's equation using Eqn 12 whereas the thinner lines relate to the Newtonian method via Eqn 27. Both sets of curves terminate at <math>p^* = p^*_{\text{arrest}} = 1 + \epsilon</math>, where <math>\epsilon = \sqrt{2\gamma r/\lambda c}</math>, with <math>c = r = 5</math>, <math>\gamma = 1/110</math>, <math>\lambda = 15/110</math> (WTC1) or <math>\lambda = 28/110</math> (WTC2). The end point for collapse occurs when the crush-front reaches the bottom of either building.</p>	32

## Figures

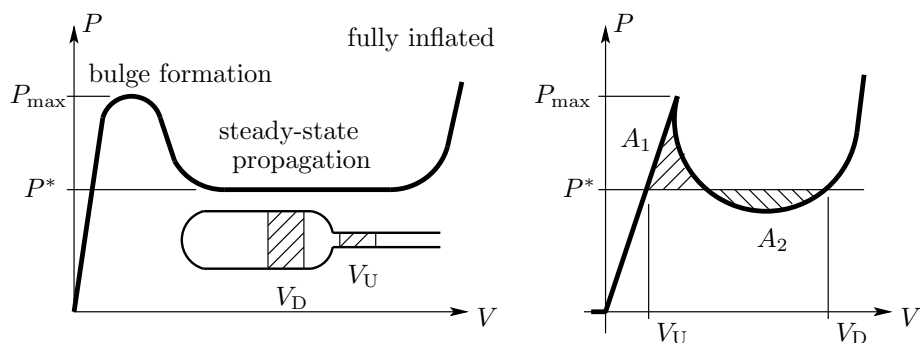


FIGURE 1: Pressure-volume response of a long, uniform party balloon. Left: the overall equilibrium path where  $V$  refers to the inflated volume. The volumes,  $V_U$  and  $V_D$ , refer to the volumes of a “unit” length of material in the undeformed region, ahead of the instability (the bulge front), and behind, after gross deformation. Right: the equilibrium response for the uniform, cylindrical inflation of the same unit length of material. The same peak pressure  $P_{\max}$  is manifest, and  $P^*$  is the steady-state force which assures propagation of the bulge, found by setting the enclosed areas,  $A_1$  and  $A_2$ , equal to each other. This procedure is known as the Maxwell Construction.

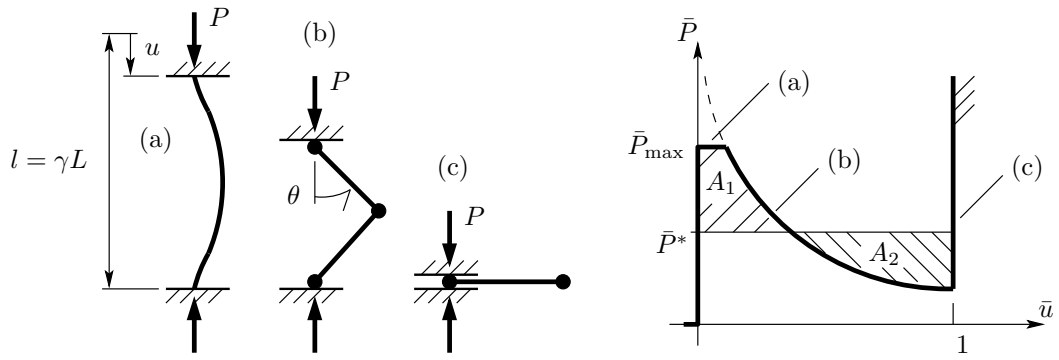


FIGURE 2: Large-displacement compression of a column built-in at both ends: (a) axial compression, which can be elastic buckling or plastic squashing, both at constant load; (b) a plastic hinge mechanism, which leads to Eqn 1; (c) a rigid contact between the ends. These stages are summarised schematically on the right in terms of a dimensionless compressive force,  $\bar{P}$ , and axial displacement,  $\bar{u}$ . The Maxwell Construction described in Fig. 1 indicates the dimensionless propagation force,  $\bar{P}^*$ , when  $A_1 = A_2$ .

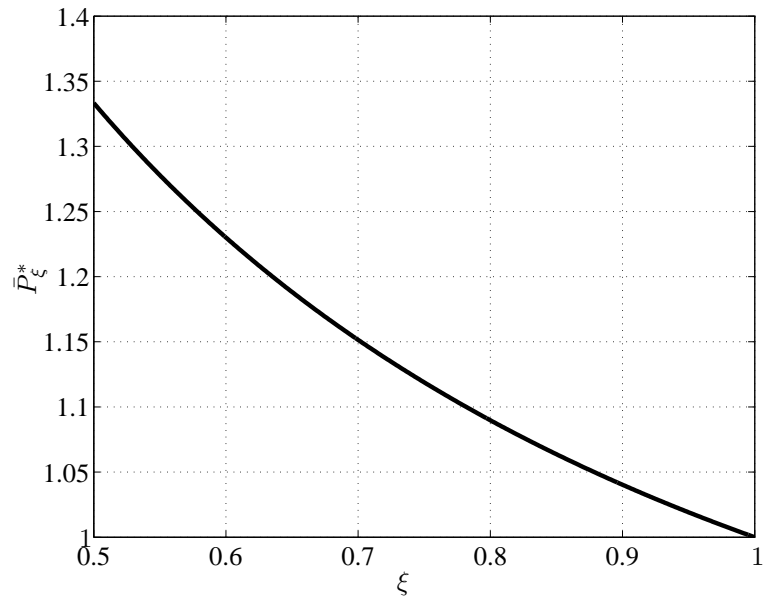


FIGURE 3: Variation of propagation force with compaction. The dimensionless force,  $\bar{P}_\xi^*$ , is the force,  $\bar{P}^*$ , from Eqn 3 divided by its value when there is full compaction, *i.e.* when  $\bar{P}^* = \pi/2$ . The dimensionless compaction ratio is  $\xi$ , which describes the relative compression of a single storey, where a value of unity is maximal:  $\xi = 0.5$  implies that the storey is compressed by 50%.

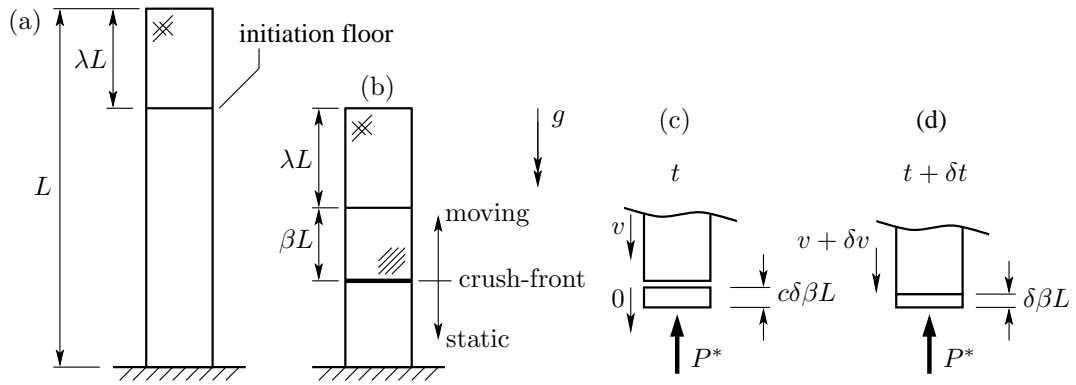


FIGURE 4: Dynamical model of progressive collapse of the overall building. (a) The initial configuration at time  $t = 0$ , where the initiation floor corresponds to the level of first damage and hence, the crush-front, located  $\lambda L$  beneath the top of the building. (b) The crush-front has propagated  $\beta L$  over time  $t$ , resulting in motion of the parts above. (c) and (d) offer incremental views of the entrainment and compression of a small element of mass over time  $\delta t$ , which acquires the velocity,  $v$ , of the falling parts. The resistance to motion is met by the propagation force,  $P^*$ , from Fig. 2, and  $c$  is a geometrical compression factor.

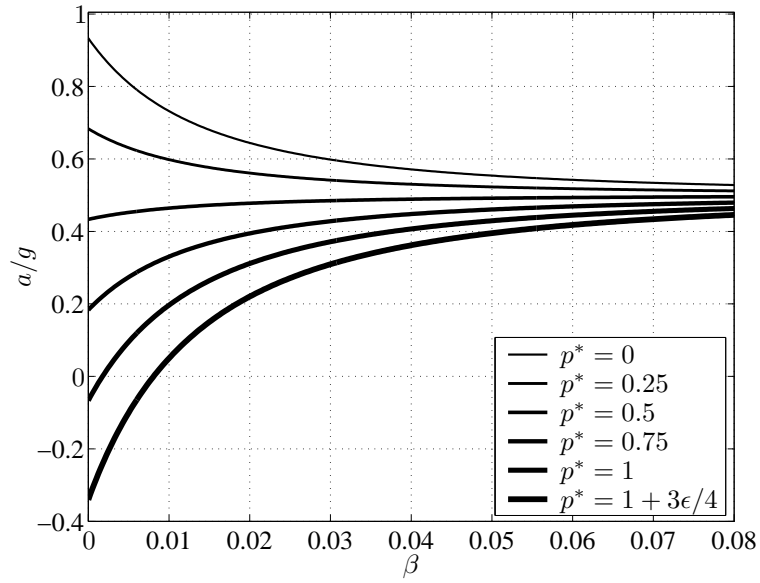


FIGURE 5: Predictions of acceleration,  $a$ , of the collapsing building above the crush-front from Fig. 4 for the indicated range of  $p^* = P^*/m_\lambda g$ , the ratio of propagation force to the weight of the initial falling part (of relative height  $\lambda = 15/110$ , as in WTC1). The final value of  $p^* = 1 + 3\epsilon/4$ , where  $\epsilon = \sqrt{2\gamma r/\lambda c}$ , is just smaller than the value to cause arrest ( $p^* = 1 + \epsilon$ ). The maximum value of  $\beta$  is  $(1 - \lambda)/c$  with  $c$  set to five.

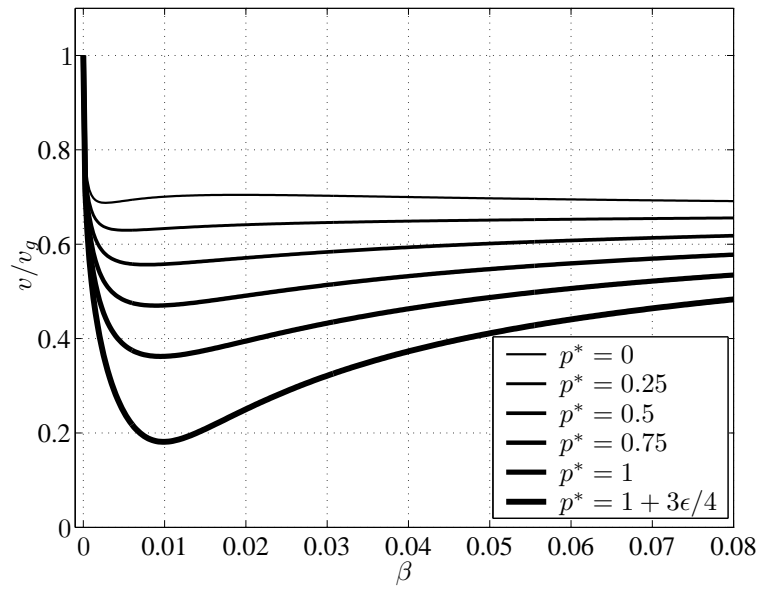


FIGURE 6: Predictions of velocity of the collapsing building above the crush-front from Fig. 4, for the same initial conditions in Fig. 5.

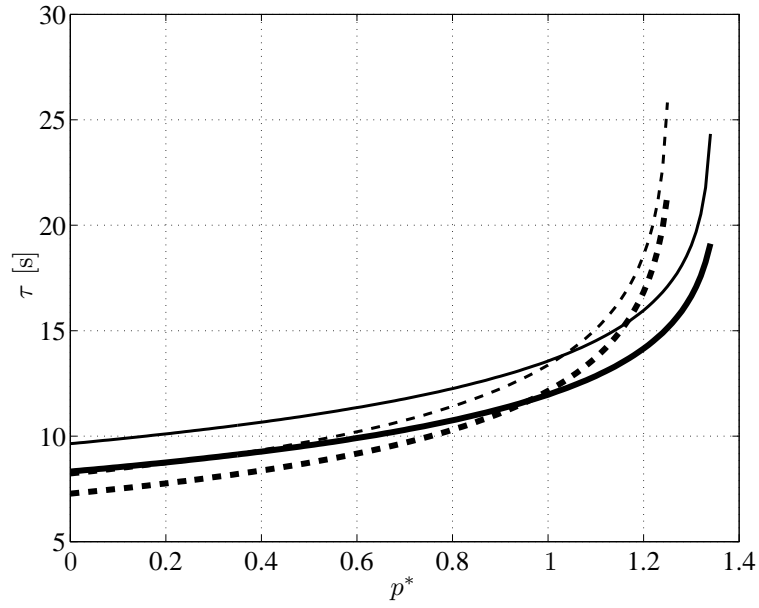


FIGURE 7: Comparison of the time period for collapse,  $\tau$ , for both WTC towers (solid, WTC1; dashed, WTC2). The thicker lines refer to solutions derived from Lagrange's equation using Eqn 12 whereas the thinner lines relate to the Newtonian method via Eqn 27. Both sets of curves terminate at  $p^* = p_{\text{arrest}}^* = 1 + \epsilon$ , where  $\epsilon = \sqrt{2\gamma r/\lambda c}$ , with  $c = r = 5$ ,  $\gamma = 1/110$ ,  $\lambda = 15/110$  (WTC1) or  $\lambda = 28/110$  (WTC2). The end point for collapse occurs when the crush-front reaches the bottom of either building.